Direct observation of thitherto unobservable quantum phenomena by using electrons

Akira Tonomura*

Advanced Research Laboratory, Hitachi, Hatoyama, Saitama 350-0395, Japan; and Frontier Research System, The Institute of Chemical and Physical Research (RIKEN), Wako, Saitama 351-0198, Japan

This contribution is part of the special series of Inaugural Articles by members of the National Academy of Sciences elected on May 2, 2000.

Contributed by Akira Tonomura, June 22, 2005

Fundamental aspects of quantum mechanics, which were discussed only theoretically as ''thought experiments'' in the 1920s and 1930s, have begun to frequently show up in nanoscopic regions owing to recent rapid progress in advanced technologies. Quantum phenomena were once regarded as the ultimate factors limiting further miniaturization trends of microstructured electronic devices, but now they have begun to be actively used as the principles for new devices such as quantum computers. To directly observe what had been unobservable quantum phenomena, we have tried to develop bright and monochromatic electron beams for the last 35 years. Every time the brightness of an electron beam improved, fundamental experiments in quantum mechanics became possible, and quantum phenomena became observable by using the wave nature of electrons.

electron microscopy | phase information | quantum mechanics

Quantum mechanics, which was born as a law describing the behavior of electrons inside atoms, now provides the basis for nearly all physical theories. However, despite the great success of quantum mechanics, it is undeniable that some phenomena still remain in the very foundation of quantum mechanics that are far beyond our conventional viewpoints. Quantum mechanics has explained many of the microscopic mechanisms of not only natural phenomena but also electronic devices in fields seeking practical applications and thus has helped open up semiconductor and other industries. Furthermore, technological developments since the 1980s have made it possible to experimentally test the fundamentals of quantum mechanics, and all of the results obtained thus far have agreed well with quantum mechanics. Quantum phenomena are thus attracting attention in applications from two sides: as obstacles to the further improvement of the performances of devices and as pathfinders for future devices.

With the aim of directly observing such quantum phenomena, electron microscopes equipped with field-emission guns that produce ever more coherent electron beams have been developed (1) so that we may precisely measure not only the intensity but also the phase of the transmitted electrons.

In this article, I present the results of the observations of my colleagues and I on the fundamentals of quantum mechanics after briefly reviewing the development of the coherent electron beams. I then describe the direct observation of the behaviors of quantum objects such as quantized vortices in superconductors by using the wave nature of electrons.

Developments of Coherent Electron Beams

As the coherence of an electron beam increases, it becomes possible to observe the wave properties of electrons in more macroscopic regions. The coherence of an electron beam can be characterized by its temporal coherence and spatial coherence (1), which increase as the beam becomes more monochromatic and more collimated, respectively. An electron of the beam is represented by a wave packet extended in the propagation direction by the temporal-coherence length and in a plane perpendicular to the propagation direction by the spatial-coherence length. It can be considered that interference takes place within this packet when parts of this packet overlap after they travel along different paths. However, because only a single electron is detected in the single event the interference pattern can be observed when similar events are accumulated.

An electron beam can be arbitrarily monochromatized for a long temporal-coherence length by passing it through an energy filter. It can also be collimated for a long spatial-coherence length, for example, by passing it through small pinholes along the beam direction. After such filtering, however, the current density is reduced significantly.

Because the beam brightness, i.e., the current density per unit of solid angle, cannot be increased by electron-optical means but is conserved by the Liouville theorem, we have to use a bright electron beam emitted by mechanisms different from conventional thermal emission. A field-emission electron gun can yield a beam several times narrower in energy spread and a few orders of magnitude greater in brightness than a thermal emission gun.

We developed a 80-kV field-emission electron beam that was brighter by two orders of magnitude (2), but we have since developed ever brighter electron beams. Every time we obtained brighter electron beams, new possibilities opened up (see Table 1). With a 250-kV microscope, we were able to measure a phase shift as small as 1/100 of an electron wavelength (3) and to carry out experiments on the Aharonov-Bohm (AB) effect (4). With 350-kV (5) and 1-MV microscopes (6), we observed in real time the dynamics of quantized vortices in both metal and high-critical temperature (T_c) superconductors (7, 8). The brightness of our most recent 1-MV electron beam increased by four orders of magnitude compared with that of the conventional 100-kV thermal beam, and the number of biprism interference fringes recordable on film increased from 300 to 11,000 (9).

Fundamental Experiments in Quantum Mechanics

New advanced technologies, such as coherent electron beams, sensitive detectors, and lithography, have made it possible to carry out fundamental experiments in quantum mechanics that once belonged to the realm of "thought experiments." I introduce two examples of results on fundamental experiments in quantum mechanics in the following.

Single-Electron Build-Up of an Interference Pattern

It was demonstrated that a two-beam interference experiment can be done in which only one electron exists at a time in the experimental apparatus and is detected one by one (10). Feynman

Freely available online through the PNAS open access option.

Abbreviations: AB, Aharonov-Bohm; T_c, critical temperature.

See accompanying Profile on page 14949.

*E-mail: tonomura@harl.hitachi.co.jp.

Table 1. History of developments of bright electron beams

Year	Electron microscope	Brightness (A/cm²·steradian)	Application results	Maximum no. of biprism fringes recordable on film
1968	100-kVTEEM	1×10^6	Experimental feasibility of electron holography	300
1978	80-kV FEEM(2)	1×10^8	Direct observation of magnetic lines of force (40)	3,000 (2)
1982	250-kVFEEM	4×10^8	Conclusive experiments of AB effect (4)	
1989	350-kVFEEM(5)	5×10^9	Dynamic observation of vortices in metal superconductors (7)	
2000	1-MV FEEM(6)	2×10^{10}	Observation of unusual behaviors of vortices in high-T_c superconductors (8, 64, 65)	11,000 (9)

TEEM, thermal-emission electron microscope; FEEM, field-emission electron microscope.

et al. (11) remarked that such an experiment would be "impossible, absolutely impossible to explain in any classical way, and has in it the heart of quantum mechanics," and they went on to say that it "has never been done in just this way, because the apparatus would have to be made on an impossibly small scale."

However, such experiments can now be carried out with our field-emission electron microscope (10). The microscope is equipped with both an electron biprism and a 2D position-sensitive electron-counting system (12) that detects individual electrons with almost 100% detection efficiency and displays their positions of arrivals as bright spots on the monitor (see Fig. 1). When the intensity of coherent electrons is high, a biprism interference pattern is soon formed with the accumulated spots.

But what happens when the intensity becomes extremely low? The bright spots signaling the electron arrivals appear to be located at random here and there at first (Fig. 2 *a* and *b*). When the number of detected electrons increases, however, the interference pattern is gradually revealed (Fig. 2 *c–e*). Even when the electron arrival rate is as low as 10 electrons per s in the entire field of view, so that at most only a single electron exists at a time in the apparatus, the interference pattern forms, although it takes an hour or so. The build-up process of an interference pattern can be viewed in Movie 1, which is published as supporting information on the PNAS web site.

Because the interference pattern is formed only when two waves simultaneously pass through on both sides of the biprism and overlap in the observation plane a single electron seems to split into two. According to the standard interpretation of quantum mechanics, even a single electron passes through both sides of the biprism in the form of the wavefunction. The two partial waves overlap to form a probability interference pattern on the observation plane. When detected, the wavefunction collapses into a single particle.

The observation results in Fig. 2 have been cited in many physics textbooks (13–17), and the experiment was selected as the first rank of the most beautiful experiments by *Physics World* (18) along with the electron interference experiment by Jönsson (19) in which actual fine two slits were used instead of the biprism.

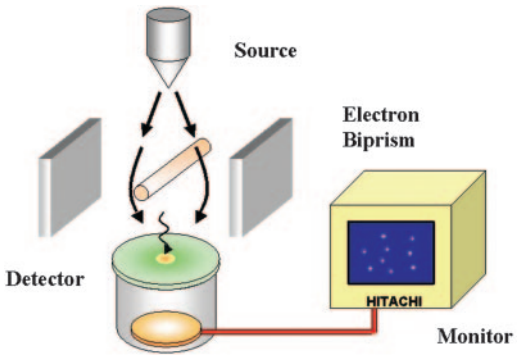

Fig. 1. Two-beam interference experiment for electrons.

Strange phenomena in quantum mechanics predictions are not limited to this double-slit experiment. Many other fundamental phenomena in quantum mechanics that contradict our classical concept have been confirmed by using neutrons (20), photons (21), and molecules (22).

The AB Effect

The apparently inexplicable behavior of electrons can also be found in the interaction of an electron wave with electromagnetic fields. The electric and magnetic fields are defined by the forces exerted on a test particle having a unit charge. However, Aharonov and Bohm (23) found cases where electrons can be physically influenced, thus producing observable effects even when they pass through only regions free of electromagnetic fields and are not subjected to any forces.

The AB effect in the magnetic case is shown in Fig. 3. Electron beams pass through on both sides of, and not through, an infinitely long solenoid and are made to overlap on the lower observation plane by the electron biprism. The interference fringes are displaced proportionally to the magnetic flux hidden inside the solenoid. It seems as if electrons are influenced by the nonlocal action of the magnetic flux at a distance. Aharonov and Bohm (23) proposed that "in quantum mechanics, the fundamental physical entities are the potentials."

The physical significance of vector potentials had been disputed over the past 150 years (24), since the days of Maxwell. The existence of the AB effect began to be questioned both theoretically (25) and experimentally (26), which led to the controversy over its existence (27). Especially in the late 1970s, when theories of gauge fields, where vector potentials were extended to gauge fields and regarded as fundamental physical entities, became the most probable candidate for unified theories of all fundamental forces of nature, the AB effect received much attention as experimental evidence that directly justified the gauge principle (28).

My colleagues and I thought that the only way to settle the seemingly endless controversy was to establish valid experimental results, so we carried out a series of experiments to do just that.

In our experiments (4, 29), we used toroidal ferromagnets instead of straight solenoids. An infinitely long solenoid is experimentally unattainable, but an ideal geometry can be achieved by using a finite system comprised of a ferromagnet with completed magnetic circuit (30, 31). In our final experiment (4), the ferromagnet was covered with a superconducting niobium layer to remove any flux leakage and any overlap of incident electrons with the magnetic fields.

Tiny complex samples were fabricated by using the most advanced lithography techniques. An electron wave was incident on a tiny toroidal sample, and the phase difference $\Delta\phi$ between

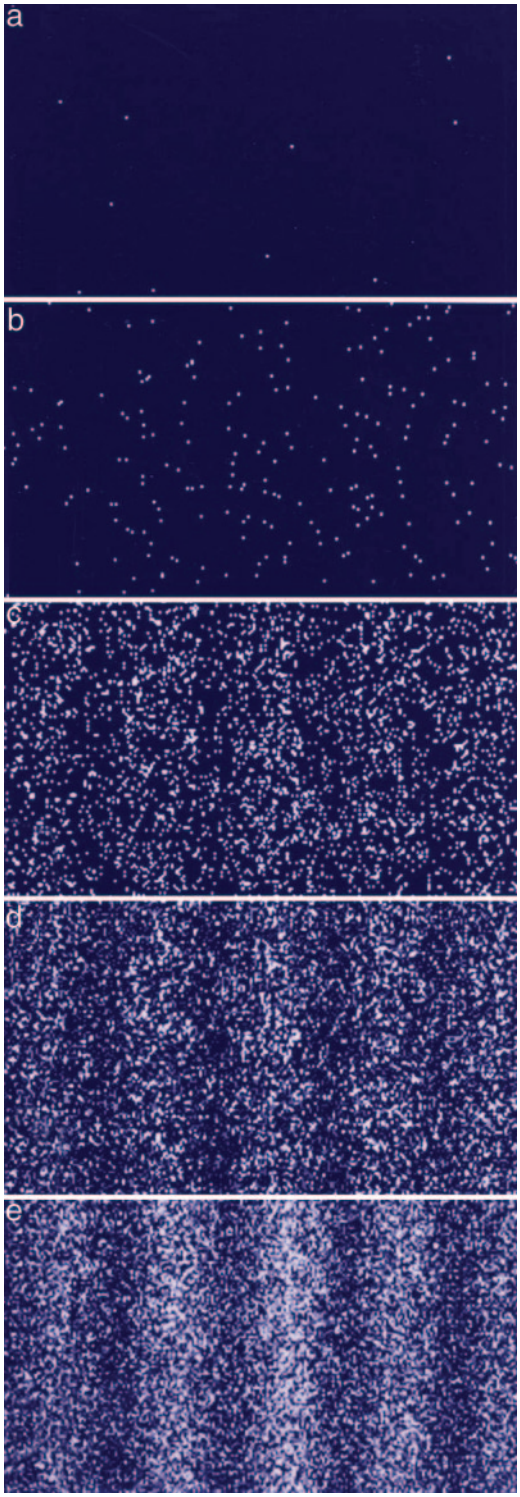

Fig. 2. Build-up of an electron interference pattern. Numbers of electrons are 10 (*a*), 200 (*b*), 6,000 (*c*), 40,000 (*d*), and 140,000 (*e*).

two waves passing through the hole and outside of the toroid was measured by interferograms.

We first confirmed within the phase precision of $2\pi/10$ that no phase difference was produced for a superconducting toroid without any magnet to eliminate the possibility that an electron wave is influenced by a superconducting torus. We also tested (32) and negated the possibility raised during the controversy

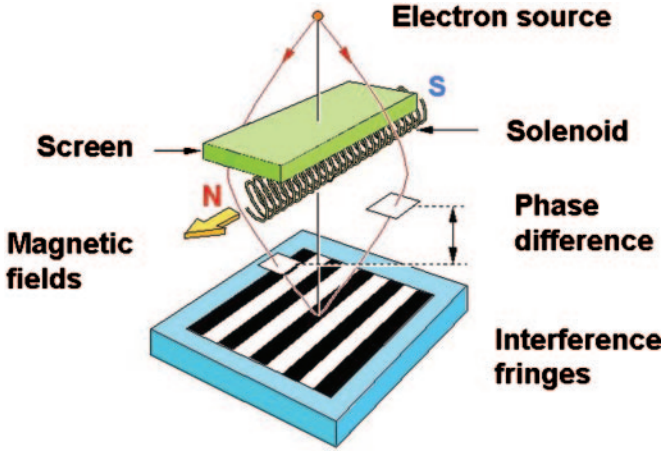

Fig. 3. The AB effect. N, north pole; S, south pole.

(33) that a minute toroidal magnetic flux might be quantized even without superconducting covering.

In our last experiment (4) concerning the AB effect using toroidal magnets covered with superconductors, we measured the $\Delta\phi$ of many samples that had various magnetic flux values. But the resultant phase difference was either 0 or π (modulo 2π). The conclusion is now obvious. The photograph in Fig. 4 indicates that a phase shift of π is produced, which indicates that the AB effect exists even when the magnetic fields are confined within the superconductor and shielded from the electron wave. When the magnetic flux surrounded by a superconductor is quantized to an odd number of $h/2e$, $\Delta\phi$ becomes π (modulo 2π). For an even number, $\Delta\phi$ is 0 (modulo 2π). Therefore, the occurrence of flux quantization was used to confirm that the niobium layer actually became superconductive, the superconductor completely surrounded the magnetic flux, and the Meissner effect prevented any flux from leaking out.

The only experimental evidence that gauge fields actually produce observable effects is the AB effect. In fact, Wu and Yang (28) describe the relation between the AB effect and gauge fields as follows.

The concept of an SU_2 gauge field was first discussed in 1954 (34). In recent years, many theorists, perhaps a majority, believe that SU_2 gauge fields do exist. However, so far there is no experimental proof of this theoretical idea, because conservation of isotopic spin only suggests, and does not require, the existence of an isotopic spin gauge field. What kind of experiment would be the definitive test of the existence of an isotopic spin gauge field? A generalized AB experiment would be.

Although the AB effect in the SU_2 gauge fields has not yet been detected despite attempts (35), the existence of the AB

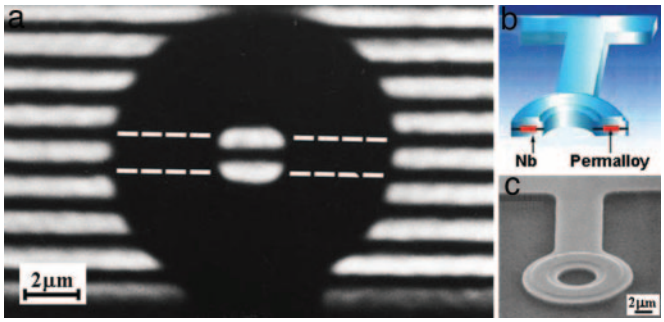

Fig. 4. Photographic evidence for the AB effect.

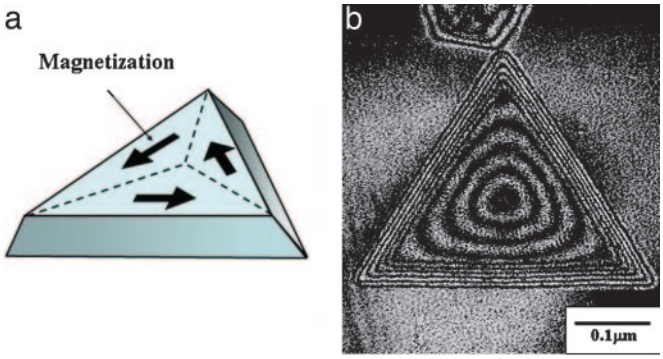

Fig. 5. Cobalt fine particle. (*a*) Schematic diagram. (*b*) Interference micrograph.

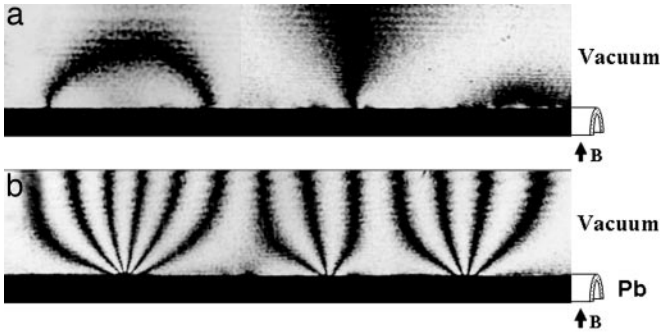

Fig. 6. Interference micrographs of magnetic lines of force penetrating thin films of lead (phase amplification: ×2). (*a*) Film thickness is 0.2 μm. (*b*) Film thickness is 1.0 μm. B indicates the applied magnetic field.

effect, or the reality of gauge fields, was conclusively confirmed by electromagnetism.

In the Yang–Mills theory (34), gauge bosons have zero masses caused by constraints of gauge invariance. Their interactions are long range, and, therefore, the existent short-range forces cannot be explained. Later, based on this gauge theory, Glashow (36), Weinberg (37), and Salam (38) unified fundamental forces by introducing spontaneous symmetry breaking, which was first proposed by Nambu and Jona-Lasinio (39). The same process by which a photon acquires a nonzero mass by symmetry breaking occurs in more common superconductors, which can now be observed with electrons, as will be described in the next section. Above T_c electrons in a superconductor are random in phase and gauge-invariant, whereas below T_c electrons form Cooper pairs and their phases are locked coherently, thus breaking the symmetry. This symmetry breaking results in a nonzero mass of a photon or the short-range nature of electromagnetic force inside a superconductor; that is, the magnetic field penetrates superconductors only shallowly. No penetration of magnetic fields into superconductors shows up as the Meissner effect and quantized vortices.

Observation of Quantum Objects

The microscopic distributions of magnetic fields have been quantitatively observed as phase contours in interference micrographs by using the AB effect principle. Interferograms, where phase shifts are represented as displacements of regular interference fringes, are directly observed with the electron biprism, but contour maps of phase shifts can be obtained through the electron holography process (40, 41), because there are no convenient Mach–Zehnder-type interferometers in electron optics: an electron hologram is formed in the electron microscope and the contour map is obtained in the optical reconstruction stage of holography with a Mach–Zehnder-type interferometer.

The phase contours in an interference micrograph of a magnetic object directly indicate magnetic lines of force in h/e flux units. When one looks at an example of a ferromagnetic fine particle (see Fig. 5), one may tend to think that some deep truth in nature may be hidden in this interaction, because the micrograph can be interpreted in such a straightforward way. Narrow fringes parallel to the edges indicate thickness contours. The circular fringes in the inner region directly indicate magnetic lines of force in $h/(2e)$ flux units, because the thickness is uniform there. The reason the flux unit is $h/(2e)$ and not h/e comes from the doubly amplified interference micrograph. This observation principle is the same as that of the superconducting flux meter, SQUID, except for the measurement flux unit. Using this method, the following observations became possible.

Quantized Magnetic Fluxes Leaking Out from Superconductors

Quantized vortices penetrating a superconductor play an important role in both the fundamental and practical applications of superconductivity. The tiny vortices play a crucial role when superconductors are put to practical use as dissipation-free electrical conductors, because they are moved by the Lorentz force caused by the current generating heat, thus eventually destroying the superconducting state. To obtain a dissipation-free current, we have to fix or pin down the vortices by material defects.

Vortices in superconductors were predicted to exist by Abrikosov (42) and were first observed by the Bitter technique (43) and more recently with other techniques (44–47). Using our method (48), we first attempted to directly observe magnetic lines of force of vortices leaking outside from a superconductor surface.

A magnetic field of a few G was applied perpendicular to a thin film of lead prepared by evaporating lead onto one side of a wire. An electron beam was incident parallel to the surfaces of films 0.2 or 1.0 μm thick, and the magnetic lines produced from the film surfaces were observed as interference micrographs (Fig. 6). The uniform magnetic lines penetrating the superconductor above T_c became localized in the form of thin vortex lines when T decreased below T_c. Because these micrographs are phase-amplified by a factor of 2, a magnetic flux of $h/(2e)$ flows between two neighboring contours. A magnetic line from a single quantized vortex can be seen in the right side of the micrograph in Fig. 6*a*. The magnetic line is produced from an extremely small area of the film surface and spreads out into free space. Because a photon acquires a nonzero mass inside superconductors caused by symmetry breaking below T_c, a magnetic field can penetrate into superconductors only for a short distance, thus forming localized thin filaments of magnetic fluxes as quantized vortices.

We also observed a pair of vortices oriented in opposite directions and connected by the magnetic lines (Fig. 6*a Left*). One possible reason for the pair's creation is that during the cooling process the film was in a state in which the vortex pair appeared and disappeared repeatedly because of thermal excitations. This phenomenon, which was predicted by the Kosterlitz–Thouless theory (49, 50), is peculiar to 2D systems. In our experiments, an antiparallel pair of vortices may have been produced during the cooling process, pinned by some imperfections in the superconductor, and eventually frozen.

What happens in a thicker film? Fig. 6*b* shows that the state of the magnetic lines is completely changed; magnetic flux penetrates the superconductor in bundles. No vortex pairs are seen.

Because lead is a type-I superconductor, a magnetic field penetrates some parts of the specimen where superconductivity

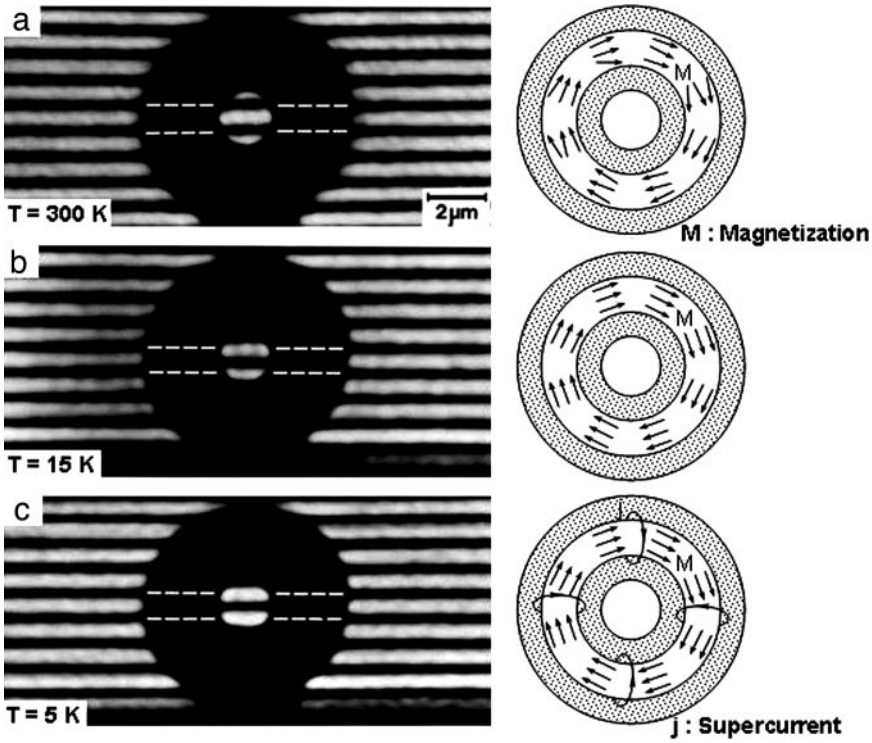

Fig. 7. Temperature dependence of interferograms of superconducting toroidal sample. (*a*) $T = 300$ K. (*b*) $T = 15$ K. (*c*) $T = 5$ K.

is destroyed ("intermediate state"). A superconducting lead film <0.5 μm thick is an exception. It behaves like a type-II superconductor, and the flux penetrates the superconductor in the form of individual vortices.

Quantization Process of Magnetic Flux

We then attempted to observe the flux quantization process directly by using toroidal ferromagnets covered with superconductors, when T decreases below T_c. C. N. Yang (31) advised us to carry out such experiments in his remarks after my talk on the AB effect at the Second International Symposium on Foundations of Quantum Mechanics. Yang wondered whether we could take a series of holograms as the temperature is lowered like Fairbank and his collaborators (51) did in their experiment of 1961. This, he surmised, would allow us to see whether flux is expelled or sucked in as the Nb becomes superconducting.

The magnetic flux enclosed in the covering superconductor must increase or decrease to take the nearest quantized values. We directly observed this process by electron interferometry. The interferograms of a toroidal ferromagnet at various temperatures are shown in Fig. 7. At 300 K, the displacement of the interference fringes is 0.25 fringe spacing. When T is decreased to 15 K, the fringe displacement increases to a 0.4 fringe spacing because of the increase ($\approx$5%) in magnetization in the permalloy. When T is further decreased and crosses T_c ($= 9.2$ K), the displacement suddenly becomes a 0.5 fringe spacing, that is, the gauge symmetry of the magnetic field is broken, and the supercurrent is induced to circulate around the ferromagnet so that the phase of the Cooper-pair wave may remain coherent, thus making the total magnetic flux quantized.

Therefore, the phase shift is either 0 or π depending on whether the number of flux quanta in the torus is even or odd. We can conclude from the geometric measurement of cross sections of permalloy ferromagnets that in the case of the present sample the magnetic flux of 8.5 ($h/2e$) at 300 K increases to 8.8 ($h/2e$) at 15 K and further increases to the nearest quantized flux value of 9 ($h/2e$) at 5 K.

Another example shows that fringe displacement of a -0.1 fringe spacing at 300 K increases to 0.15 fringe spacing at 15 K and then decreases to zero because of the supercurrent flowing in the opposite direction. As these examples show, when T crosses below T_c, the nearest quantized value is selected as the quantized flux value. We can now directly look at flux quantization, the result of symmetry breaking, when T crosses below T_c.

Dynamic Observation of Vortices Inside Superconductors

Up to now we have observed hidden quantized magnetic fluxes enclosed by covering superconductors as displacements of electron interference fringes outside of the superconductors and also magnetic lines of vortices leaking out from superconductor surfaces. To observe vortices inside superconductors and pinning centers directly, we developed a method that uses the phase of electrons transmitted through superconducting thin films. In this method, magnetic lines of vortices inside superconductors can also be observed by interference microscopy (52). When we want to observe the dynamics of vortices, however, it is more suitable to use out-of-focus imaging (7). The phase distribution cannot be observed in the in-focus image, where only the intensity distribution is observed. However, when the image is defocused spatial changes in the phase distribution are transformed into the corresponding changes in the intensity distribution. This out-of-focus imaging method called "Lorentz microscopy" has been used for the observation of magnetic domain structures in ferromagnetic thin films. Lorentz microscopy for vortex observation has become feasible with a bright field-emission electron beam, which enables highly collimated illumination of electrons onto the sample films, and thus opened a way to directly observe the motion of vortices relative to pinning centers in real time and microscopically investigate the pinning and depinning mechanisms of vortices.

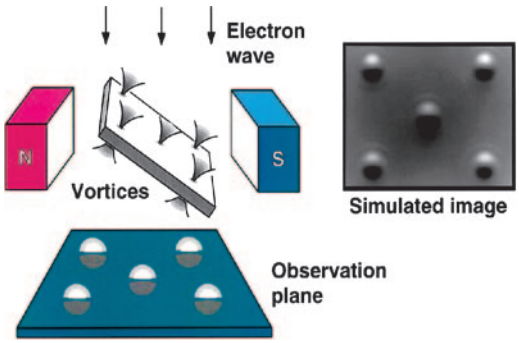

Fig. 8. Principle behind vortex observation, Lorentz microscopy. N, north pole; S, south pole.

The experimental arrangement is shown in Fig. 8. Electrons passing through a tilted superconducting thin film are phase-shifted by the magnetic fields of the vortices. A vortex can be visualized as a spot consisting of a pair of bright and dark contrast features.

Using this method, we observed in real time the motion of vortices in Nb thin films under various conditions of the film temperatures and the magnetic fields applied to the films. We observed that the static configurations of vortices were various, especially depending on the conditions of the distributions and strengths of pinning centers, and that their motions also showed a rich variety of plastic flows where vortices moved at different velocities in different parts (53). To cite concrete examples, vortices usually form closely packed lattices without any pinning centers and begin to flow as a whole in the lattice form when a driving force is applied. Whereas with pinning centers, vortices cannot form a single-crystalline lattice. When weak pinning centers exist sparsely, defects in a vortex lattice such as dislocations are often produced. In this case, vortices flow almost in the form of a perfect lattice and the dislocations move across the flow. When strong pinning centers exist, vortices form grains of lattices with boundaries, because some vortices are strongly fixed by the pinning centers. They begin to flow not in the form of a perfect lattice but just like an intermittent river flows along the domain boundaries.

Vortices behave in especially interesting manners when a regular array of artificial point defects are formed in the films. It is known that the critical current of such a superconductor has peaks at specific values of the applied magnetic field. We investigated the microscopic mechanism of this peak effect by using a Nb thin film with a square array of point defects (54).

The resultant Lorentz micrographs are shown in Fig. 9. At the "matching" magnetic field H_1 in Fig. 9*b*, all of the defects are occupied by vortices without any vacancies, thus forming a square lattice. The peak effect can be explained as follows: when vortices form a regular and rigid lattice, even if a vortex is depinned from one pinning site assisted by thermal excitation, it cannot find any vacant site to move to. As a result, a bigger driving force is needed for the depinning, because other surrounding vortices also have to be moved.

Vortices form regular lattices at the matching magnetic field and its integral multiples and their integral fractions, i.e., at $H = mH_1/n$ (m, n: integers). Examples of the cases of $H = 4\,H_1$ and $H = (1/4)H_1$ are shown in Fig. 9 *a* and *c*.

The pinning force becomes stronger as a whole at specific magnetic fields, while "excess" or "deficient" vortices produced at magnetic fields different from the specific values can be induced to hop by a weaker force, just like the "electrons" and "holes" in semiconductors.

The dynamics of the vortices in periodic pinning arrays is also interesting. The vortices show quite different kinds of flow depending on the values of H, such as individual hopping among vacant interstitial sites when pinning sites are fully occupied but interstitial sites are not fully occupied by vortices, and simultaneous movements along lines of interstitial sites when these interstitial site are also fully occupied by vortices (see Movie 2, which is published as supporting information on the PNAS web site).

Especially impressive was the dynamic observation of the vortex-pair annihilation that reminds us of the pair annihilation of particles and antiparticles in accelerator experiments. We found unexpectedly that antivortices were produced in commonplace processes, such as in magnetization measurements, and had a great influence on vortex pinning (55).

For example, antivortices were produced in the following process: when the magnetic field applied to a Nb thin film was suddenly switched off 90% of the vortices left the film instantly and 10% remained pinned at weak pinning centers in the film. But the remaining 10% gradually left the film from its nearest edge, hopping from one pinning center to another by thermal excitation. When we applied the magnetic field in the opposite direction and gradually increased it, the original vortices began to leave the film faster. However, antivortices soon began to be produced from the edge of the film and to hop in the opposite direction, i.e., toward the inner region of the film. Where two streams of vortices and antivortices collided head on, the antiparallel pairs at the heads of the two streams annihilated each other one after another.

Fig. 10 shows two frames from Movie 3, which is published as supporting information on the PNAS web site, one just before the pair annihilation and the other just after. When these two annihilated each other, the next vortex–antivortex pair approached by hopping and annihilated each other. Macroscopic measurements provide no clues as to what is happening because the total magnetic flux in this field of view remains zero when vortices and antivortices are equal in number.

Antivortices have a dramatic effect on vortex pinning in some cases, for example, when strong pinning centers exist only locally in a superconductor. In fact, when a magnetic field was applied

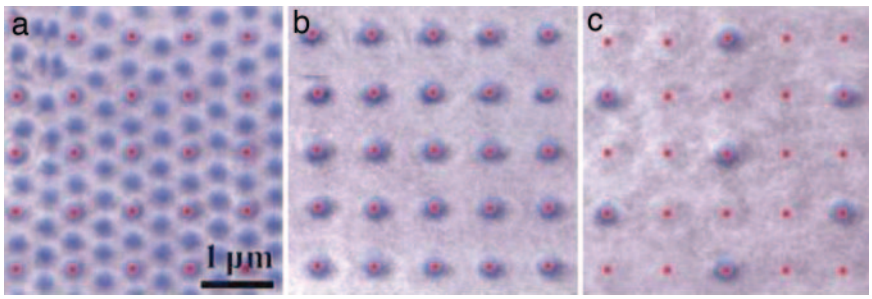

Fig. 9. Lorentz micrographs of the vortices in Nb thin film with a square array of point defects at magnetic fields. (*a*) $H = 4\,H_1$. (*b*) $H = H_1$. (*c*) $H = (1/4)\,H_1$.

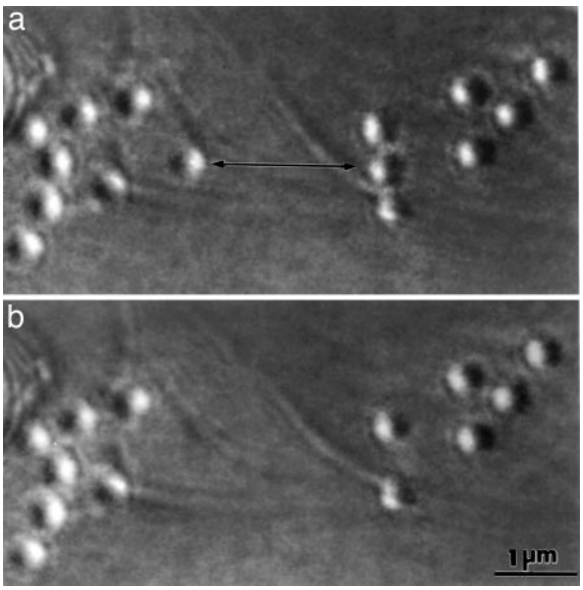

Fig. 10. Annihilation of antiparallel pair of vortices. (*a*) Before annihilation. (*b*) After annihilation.

to a film to produce vortices and then decreased only the unpinned vortices quickly left the film. Because vortices were trapped only locally in a region where pinning centers existed antivortices began to be produced in a region where no pinning centers existed. The produced antivortices were attracted toward the trapped vortices, and the vortex pairs disappeared by the head-on collision. The annihilation of a trapped vortex and an incoming antivortex is equivalent to the depinning of the trapped vortex. It is thus clarified that vortices can easily be depinned even from strong pinning centers by the pair annihilation process.

A quantized vortex is an example of the topological defects that appear in various areas in physics, such as cosmic strings in the early universe, vortices in superfluid helium, and lattice defects in liquid and solid crystals. The vivid dynamic scenes showing various processes of the pair annihilation allow our imagination its full play, making it possible, for example, to envision how antimatter moves to annihilate matter in accelerator experiments.

Our experiments can be regarded as model experiments in other fields of physics just as the superfluid-helium experiments proposed by Zurek (56) can be regarded as model experiments of cosmic-string formation in the early universe. A growing interest is focused on what happens when an electric current is applied to such vortex pairs. Because they receive additional Lorentz forces in opposite directions perpendicular to the current, the pair will not be annihilated by a simple head-on collision. Under appropriate conditions, the vortex and the antivortex may begin to rotate around each other. Vortices are strings and therefore such experiments may simulate a special kind of collision between two opposite cosmic strings.

Winding Vortex Lines in High-T_c Superconductors

Vortices in high-T_c superconductors tend to wiggle because of the anisotropic layered structures of materials and show interesting behavior. To investigate the 3D arrangements of the vortices inside the superconductors and their dynamic behaviors, we developed a 1-MV field-emission electron microscope (6), because we needed electron beams that could penetrate a film thicker than the large magnetic radius (penetration depth) of vortices in high-T_c superconductors.

We first investigated the static and dynamic behaviors of the vortices at columnar defects. Once it became possible to distinguish two different arrangements of vortices inside superconductors, a vortex trapped along a tilted column and a vortex penetrating the film perpendicularly, as two different images (8), we investigated the different pinning behaviors of these two kinds of vortices under various conditions. For example, when a driving force was applied, only untrapped vortices soon began to move.

We also used this 1-MV electron microscope to solve the mysterious arrangements of vortices peculiar to high-T_c superconductors. Vortices usually form a closely packed triangular lattice. When the magnetic field is strongly tilted away from the *c* axis, however, it was found by using the Bitter technique that the vortices form arrays of linear chains, which are far from being closely packed in case of $YBaCu_3O_{7.8}$ (YBCO) (57). Large free spaces exist between chains. In the case of Bi-2212 (58, 59), alternating domains of chains and triangular lattices are formed. Although the chain state in YBCO has been theoretically explained by the tilting of vortex lines within the framework of the anisotropic London theory (60), no experimental evidence was obtained for it. The chain-lattice state in Bi-2212 had long been a topic of discussion.

Koshelev (61) proposed an interesting model for the chain-lattice state in Bi-2212 that assumes two sets of vortices perpendicular to each other: Josephson vortices penetrate between the layer planes in the form of elliptical vortices, and pancake vortices (62) penetrate the film perpendicularly to the layer plane. Vortices crossing the Josephson vortices attract each other, thus forming chains (63). The rest of the vortices form triangular lattices.

We used our method to determine whether vortex lines in the chain states inside high-T_c superconductors are tilted. In the case of $YBaCu_3O_{7.8}$, the conclusion is evident from the obtained

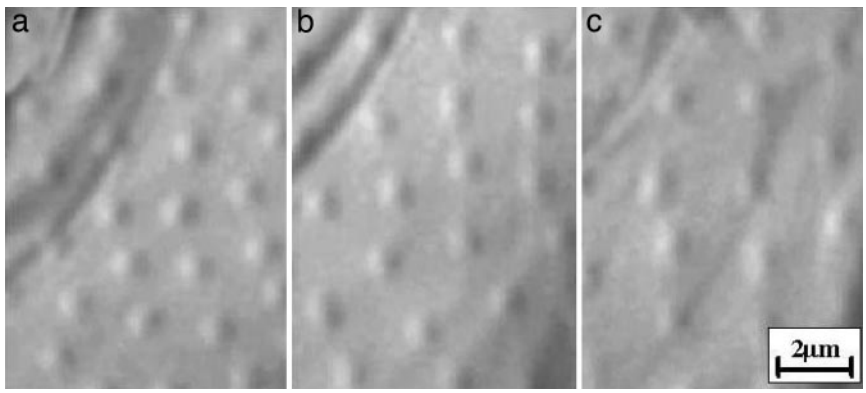

Fig. 11. Lorentz micrographs of vortices in a $YBaCu_3O_{7.8}$ film sample at tilted magnetic fields ($T = 30$ K). (*a*) $\theta = 75°$. (*b*) $\theta = 82°$. (*c*) $\theta = 83°$.

Lorentz micrographs (64) in Fig. 11. These micrographs show that as the tilting angle of the magnetic field increases the vortex images become more elongated, indicating the tilting of vortex lines and formation of linear chains. In the case of Bi-2212, Lorentz microscopy observation showed that neither chain nor lattice vortices tilted. Instead, both types stood perpendicular to the layer plane (64), which supported the Koshelev model.

We also found unexpected results. Images of chain vortices began to disappear at lower temperatures than T_c (65). We interpret this phenomena to be caused by incommensurate chain vortices oscillating along the chain direction caused by thermal vibration of vortices.

Conclusion

Thanks to the recent development of advanced technologies, experiments that were once regarded as thought experiments in quantum mechanics can now be carried out. In addition, the wave nature of electrons allows us to observe previously unobservable microscopic objects. Examples are the observation of microscopic distribution of magnetic lines of force in h/e units and the dynamics of quantized vortices in superconductors. This measurement and observation technique is expected to play a more important role in future research and development in nanoscience and nanotechnology.

1. Tonomura, A. (1999) *Electron Holography* (Springer, Heidelberg), 2nd Ed.
2. Tonomura, A., Matsuda, T., Endo, J., Todokoro, H. & Komoda, T. (1979) *J. Electron Microsc.* **28,** 1–11.
3. Tonomura, A., Matsuda, T., Kawasaki, T., Endo, J. & Osakabe, N. (1985) *Phys. Rev. Lett.* **54,** 60–62.
4. Tonomura, A., Osakabe, N., Matsuda, T., Kawasaki, T., Endo, J., Yano, S. & Yamada, H. (1986) *Phys. Rev. Lett.* **56,** 792–795.
5. Kawasaki, T., Matsuda, T., Endo, J. & Tonomura, A. (1990) *Jpn. J. Appl. Phys.* **29,** L508–L510.
6. Kawasaki, T., Yoshida, T., Matsuda, T., Osakabe, N., Tonomura, A., Matsui, I. & Kitazawa, K. (2000) *Appl. Phys. Lett.* **76,** 1342–1344.
7. Harada, K., Matsuda, T., Bonevich, J., Igarashi, M., Kondo, S., Pozzi, G., Kawabe, U. & Tonomura, A. (1992) *Nature* **360,** 51–53.
8. Tonomura, A., Kasai, H., Kamimura, O., Matsuda, T., Harada, K., Nakayama, Y., Shimoyama, J., Kishio, K., Hanaguri, T., Kitazawa, K., *et al*. (2001) *Nature* **412,** 620–622.
9. Akashi, T., Harada, K., Matsuda, T., Kasai, H., Tonomura, A., Furutsu, T., Moriya, M., Yoshida, T., Kawasaki, T., Kitazawa, K., *et al*. (2002) *Appl. Phys. Lett.* **81,** 1922–1924.
10. Tonomura, A., Endo, J., Matsuda, T., Kawasaki, T. & Ezawa, H. (1989) *Am. J. Phys.* **57,** 117–120.
11. Feynman, R. P., Leighton, R. B. & Sands, M. (1965) *The Feynman Lectures on Physics* (Addison–Wesley, Reading, MA), Vol. III, pp. 1.1–1.5.
12. Tsuchiya, Y., Inuzuka, E., Kurono, T. & Hosoda, M. (1985) *Adv. Electron. Electron Phys.* **64,** 21–31.
13. Tipler, P. A. (1999) *Physics* (Freeman Worth, New York), 4th Ed., pp. 509–510.
14. Bransden, B. H. & Joachain, C. J. (2000) *Quantum Mechanics* (Pearson Education, Essex, U.K.), 2nd Ed., pp. 53–54.
15. Giancoli, D. C. (1995) *Physics* (Prentice–Hall, Englewood Cliffs, NJ), 4th Ed., pp. 806–807.
16. Ezawa, H. (2002) *Quantum Mechanics (I)* (Syokabo, Tokyo), pp. 71–74.
17. Hara, Y. (2004) *Fundamentals of Physics* (Gakujyutsu Syuppan, Tokyo), 3rd Ed., p. 300.
18. Crease, R. P. (2002) *Phys. World* **15,** 19–20.
19. Jönsson, C. (1961) *Physik* **161,** 454–474.
20. Rauch, H. & Werner, S. A. (2000) *Neutron Interferometry* (Oxford Univ. Press, New York).
21. Aspect, A., Gragier, P. & Roger, G. (1981) *Phys. Rev. Lett.* **47,** 460–463.
22. Arndt, M., Nairz, O., Vos-Andreae, J., Keller, C., van der Zouw, G. & Zeilinger, A. (1999) *Nature* **401,** 680–682.
23. Aharonov, Y. & Bohm, D. (1959) *Phys. Rev.* **115,** 485–491.
24. Yang, C. N. (1996) in *Quantum Coherence and Decoherence*, eds. Fujikawa, K. & Ono, Y. A. (Elsevier, Amsterdam), pp. 307–314.
25. Bocchieri, P. & Loinger, A. (1978) *Nuovo Cimento* **47A,** 475–482.
26. Roy, S. M. (1980) *Phys. Rev. Lett.* **44,** 111–114.
27. Peshkin, M. & Tonomura, A. (1989) *The Aharonov-Bohm Effect: Lecture Notes in Physics* (Springer, Heidelberg).
28. Wu, T. T. & Yang, C. N. (1975) *Phys. Rev. D* **12,** 3845–3857.
29. Tonomura, A., Matsuda, T., Suzuki, R., Fukuhara, A., Osakabe, N., Umezaki, H., Endo, J., Shinagawa, K., Sugita, Y., Fujiwara, H., *et al*. (1982) *Phys. Rev. Lett.* **48,** 1443–1446.
30. Kuper, C. G. (1980) *Phys. Lett.* **79,** 413–416.
31. Yang, C. N. (1986) in *Proceedings of the Second International Symposium on Foundations of Quantum Mechanics*, eds. Namiki, M., Ohnuki, Y., Murayama, M. & Nomura, S. (Physical Society of Japan, Tokyo), p. 105.
32. Tonomura, A., Umezaki, H., Matsuda, T., Osakabe, N., Endo, J. & Sugita, Y. (1983) *Phys. Rev. Lett.* **51,** 331–334.
33. Costa de Beauregard, O. & Vigourex, J. M. (1982) *Lett. Nuovo Cimento* **33,** 79–80.
34. Yang, C. N. & Mills, R. (1954) *Phys. Rev.* **96,** 191–195.
35. Greenberger, D. M., Atwood, D. K., Arthur, J., Shull, C. G. & Schlenker, M. (1981) *Phys. Rev. Lett.* **47,** 751–754.
36. Glashow, S. L. (1980) *Rev. Mod. Phys.* **52,** 539–543.
37. Weinberg, S. (1967) *Phys. Rev. Lett.* **19,** 1264–1266.
38. Salam, A. (1968) *in Elementary Particle Theory*, ed. Svartholm, N. (Almguest & Wiksells, Stockholm), pp. 367–377.
39. Nambu, Y. & Jona-Lasinio, G. (1961) *Phys. Rev.* **122,** 345–358.
40. Tonomura, A., Matsuda, T., Endo, J., Arii, T. & Mihama, K. (1980) *Phys. Rev. Lett.* **44,** 1430–1433.
41. Tonomura, A. (1987) *Rev. Mod. Phys.* **59,** 637–669.
42. Abrikosov, A. A. (1957) *Soviet Phys. JETP* **5,** 1174–1182.
43. Essman, U. & Träuble, H. (1967) *Phys. Lett.* **24,** 526–527.
44. Hess, H. F., Robinson, R. B. & Waszczak, J. V. (1990) *Phys. Rev. Lett.* **64,** 2711–2714.
45. Chang, A. M., Hallen, H. D., Harriott, L., Hess, H. F., Kao, H. L., Kwo, J., Miller, R. E., Wolfe, R., van der Ziel, J. & Chang, T. Y. (1992) *Appl. Phys. Lett.* **61,** 1974–1976.
46. Vu, L. N., Wistrom, M. S. & Van Harlingen, D. J. (1993) *Appl. Phys. Lett.* **63,** 1693–1695.
47. Goa, P. E., Hauglin, H., Baziljevich, M., Il'yashenko, E., Gammel, L. & Johansen, T. H. (2001) *Supercond. Sci. Technol.* **14,** 729–731.
48. Matsuda, T., Hasegawa, S., Igarashi, M., Kobayashi, T., Naito, M., Kajiyama, H., Endo, J., Osakabe, N., Tonomura, A. & Aoki, R. (1989) *Phys. Rev. Lett.* **62,** 2519–2522.
49. Kosterlitz, J. M. & Thouless, D. J. (1973) *J. Phys.* **6,** 1181–1203.
50. Halperin, B. I. & Nelson, R. (1979) *J. Low Temp. Phys.* **36,** 599–616.
51. Deaver, B. S., Jr., & Fairbank, W. M. (1961) *Phys. Rev. Lett.* **7,** 43–46.
52. Bonevich, J. E., Harada, K., Matsuda, T., Kasai, H., Yoshida, T., Pozzi, G. & Tonomura, A. (1993) *Phys. Rev. Lett.* **70,** 2952–2955.
53. Crabtree, G. W. & Nelson, D. R. (1997) *Phys. Today* **50,** 38–45.
54. Harada, K., Kamimura, O., Kasai, H., Mastuda, T. & Tonomura, A. (1996) *Science* **274,** 1167–1169.
55. Harada, K., Kasai, H., Matsuda, T., Yamasaki, M. & Tonomura, A. (1997) *J. Electron Microsc.* **46,** 227–232.
56. Zurek, W. H. (1985) *Nature* **317,** 505–508.
57. Gammel, P. L., Bishop, D. J., Rice, J. P. & Ginsbreg, D. M. (1992) *Phys. Rev. Lett.* **68,** 3343–3346.
58. Bolle, C. A., Gammel, P. L., Grier, D. G., Murray, C. A., Bishop, D. J., Mitzi, D. B. & Kapitulnik, A. (1991) *Phys. Rev. Lett.* **66,** 112–115.
59. Grigorieva, I. V. & Steeds, J. W. (1995) *Phys. Rev. B* **51,** 3765–3771.
60. Buzdin, A. & Simonov, A. (1990) *JETP Lett.* **51,** 191–195.
61. Koshelev, A. E. (1999) *Phys. Rev. Lett.* **83,** 187–190.
62. Clem, J. R. (1991) *Phys. Rev. B* **43,** 7837–7846.
63. Buzdin, A. & Baladie, I. (2002) *Phys. Rev. Lett.* **88,** 147002.
64. Tonomura, A., Kasai, H., Matsuda, T., Harada, K., Yoshida, T., Akashi, T., Shimoyama, J., Kishio, K., Hanaguri, T., Kitazawa, K., *et al*. (2002) *Phys. Rev. Lett.* **88,** 237001.
65. Matsuda, T., Kamimura, O., Kasai, H., Harada, K., Yoshida, T., Akashi, T., Tonomura, A., Nakayama, Y., Shimoyama, J., Kishio, K., *et al*. (2001) *Science* **294,** 2136–2138.